Enhanced Channel Hardening-Exploiting Message Passing Algorithm For Large-scale MIMO Detection

Chuang Yang, Leiming Tang and Zheng Wang
Nanjing University of Aeronautics and Astronautics, Nanjing, China
Email:{chuangyang, leiming, z.wang}@nuaa.edu.cn

2021 IEEE Wireless Communications and Networking Conference (WCNC) | 978-1-7281-9505-6/20/$31.00 ©2021 IEEE | DOI: 10.1109/WCNC49053.2021.9417571

***Abstract*—In this paper, the enhanced channel hardening-exploiting message passing (ECHEMP) algorithm is proposed for large-scale MIMO detection to improve the decoding performance with less complexity cost, so as to a better decoding trade-off. Specifically, the proposed algorithm consists of two stages. In the first stage, to enhance the convergence performance of the iterative detection symbols estimation, we propose to use the discrete Gaussian distribution rather than the uniform one as the default initial probability distribution, and give the initial estimation as the mean of the discrete Gaussian distribution under channel hardening phenomenon. In the second stage, compared to iterative calculations of all detection symbols, the number of calculations of detection symbols in the iterative process is reduced through a probability threshold, which efficiently reduces computational complexity. Finally, simulation results about MIMO detection are presented to verify the performance improvement and the complexity reduction.**

***Index Terms*—Large-scale MIMO systems, message passing detector, iterative detection, channel hardening**

I. Introduction

Large-scale multi-input multi-output (MIMO) system is a rising technology in 5G that promises remarkable improvements in terms of energy efficiency, power consumption and link reliability compared to conventional MIMO system [1]. However, realizing a massive MIMO system faces numerous challenges. A pressing challenge among them lies in the uplink signal detection for a massive MIMO system, where it is difficult to achieve a reasonable compromise between low computational load and good detection accuracy. When the number of antennas at base station is much larger than the number of uplink users, minimum mean square error (MMSE) turns out to be a promising detection solution by achieving near-optimal performance with polynomial complexity $O(n^3)$ [2]. However, MMSE detection involves complicated matrix inversions and multiplications, resulting in low processing efficiency in practice. To reduce the computational complexity, numerous methods have been proposed to avoid the inverse of the matrix, such as Neumann Series Expansion, Gauss-Seidel, Chebyshev iteration and Conjugate gradient [3]–[5].

Recently, message passing detection (MPD) algorithm which is matrix-inverse free, has attracted a lot of research attentions [6]. Among them, the channel hardening-exploiting message passing (CHEMP) algorithm has been proposed in [7]. It simplifies the calculation of the Gram matrix and approximates the interference-plus-noise to a Gaussian distribution, thus leading to a better performance than MMSE detector. Then, a number of low complexity CHEMP algorithms are proposed [8]–[10]. Specifically, the probability approximation message passing detection (PA-MPD) algorithm in [8] chooses a part of the symbol probabilities to calculate the messages in each iteration. The low complexity message passing detection (LCMPD) algorithm in [10] avoids exponential operation or division. However, these low complexity algorithms achieve the complexity reduction at the expense of decoding performance.

In this paper, the enhanced CHEMP (ECHEMP) algorithm is proposed for large-scale MIMO detection, which not only reduces the computational load, but also improves the decoding performance. In particular, the proposed ECHEMP algorithm consists of two stages. In the first stage, in order to improve the convergence performance of detection symbols, the discrete Gaussian distribution is used to optimize the initial probability distribution of detection symbols. The mean of the discrete Gaussian distribution is estimated by the approximation matrix under channel hardening phenomenon. This is different from the general cases in [8]–[10], where a uniform initial probability distribution for detection symbols is set. In the second stage, the approximated probability updating mechanism is adopted to reduce the computational complexity. More precisely, a probability threshold is set to effectively reduce the number of detection symbols at each iteration.

II. System Model

We consider a MIMO system with K transmit antennas and N receive antennas. The input-output relationship is given by

$$\tilde{\mathbf{y}} = \tilde{\mathbf{H}}\tilde{\mathbf{x}} + \tilde{\mathbf{n}}. \tag{1}$$

Let $\tilde{\mathbf{x}} = [\tilde{x}_1, \tilde{x}_2, ..., \tilde{x}_K]^T$ denote the transmitted symbol vector, where each element $\tilde{x}_i$ is a M-quadrature amplitude modulation (M-QAM) symbol. $\tilde{\mathbf{y}} = [\tilde{y}_1, \tilde{y}_2, ..., \tilde{y}_N]^T$ is the received signal vector in the base station (BS). $\tilde{\mathbf{H}}$ denotes the channel gain matrix. The channel gain $\tilde{H}_{ij}$ is assumed to follow independent Gaussian distribution with zero mean and variance $\sigma_j^2 = 1$. The entries of $\tilde{\mathbf{n}}$ are i.i.d. complex Gaussian with variance σ_n^2 each.

Clearly, the system model in (1) can be written in the real-valued model

$$\mathbf{y} = \mathbf{H}\mathbf{x} + \mathbf{n} \tag{2}$$

with $\mathbf{H} = \left[\mathcal{R}(\tilde{\mathbf{H}})\ -\mathcal{I}(\tilde{\mathbf{H}});\ \mathcal{I}(\tilde{\mathbf{H}})\ \mathcal{R}(\tilde{\mathbf{H}})\right] \in \mathbb{R}^{2N\times 2K}$, $\mathbf{y} =$

Corresponding author: Zheng Wang(e-mail: z.wang@nuaa.edu.cn)

$\begin{bmatrix}\mathcal{R}(\tilde{\mathbf{y}});\ \mathcal{I}(\tilde{\mathbf{y}})\end{bmatrix} \in \mathbb{R}^{2N}$, $\mathbf{x} = \begin{bmatrix}\mathcal{R}(\tilde{\mathbf{x}});\ \mathcal{I}(\tilde{\mathbf{x}})\end{bmatrix} \in \mathbb{R}^{2K}$, $\mathbf{n} = \begin{bmatrix}\mathcal{R}(\tilde{\mathbf{n}});\ \mathcal{I}(\tilde{\mathbf{n}})\end{bmatrix} \in \mathbb{R}^{2N}$, where $\mathcal{R}(.)$ and $\mathcal{I}(.)$ denote the real and imaginary parts, respectively. Let $\mathcal{X} = \{s_1, s_2, ..., s_{\sqrt{M}}\}$ denote the set of real value constellation points under M-QAM.

Given (2), the minimum mean square error (MMSE) detection is obtained by

$$\mathbf{x} = (\mathbf{H}^T\mathbf{H} + \sigma_n^2\mathbf{I})^{-1}\mathbf{H}^T\mathbf{y}, \tag{3}$$

Because MMSE detector need to calculate matrix inversion, the CHEMP algorithm is proposed as a low complexity detector [7]. In particular, by multiplying both sides of (2) by $\mathbf{H}^T$ and divides by N, the system model in (2) becomes

$$\mathbf{z} = \mathbf{J}\mathbf{x} + \mathbf{v} \tag{4}$$

with $\mathbf{z} = \mathbf{H}^T\mathbf{y}/N$, $\mathbf{J} = \mathbf{H}^T\mathbf{H}/N$ and $\mathbf{v} = \mathbf{H}^T\mathbf{n}/N$. More specifically, the ith element of $\mathbf{z}$ is

$$z_i = J_{ii}x_i + g_i \tag{5}$$

with

$$g_i = \sum_{j=1, j\neq i}^{2K} J_{ij}x_j + v_i. \tag{6}$$

In order to detect the symbol $x_j, 1 \leq j \leq 2K$ in $\mathbf{x}$, the probabilities $p(x_j = s_k), 1 \leq k \leq \sqrt{M}$ are calculated in an iterative way, where the detected result $\widehat{x}_j$ is determined by

$$\widehat{x}_j = \max_{s_k \in \mathcal{X}} p(x_j = s_k). \tag{7}$$

Specifically, to calculate $p(x_j = s_k)$, the CHEMP algorithm firstly computes the expectation and the variance of g_i as

$$\mu_i^{(t)} = \mathbb{E}(g_i) = \sum_{j=1, j\neq i}^{2K} J_{ij}\mathbb{E}^{(t)}(x_j), \tag{8}$$

$$\sigma_i^{2(t)} = \mathrm{Var}(g_i) = \sum_{j=1, j\neq i}^{2K} J_{ij}^2\mathrm{Var}^{(t)}(x_j) + \sigma_v^2, \tag{9}$$

where t is the index of iteration and $\sigma_v^2 = \sigma_n^2/(2N)$. Here, a uniform initial distribution is applied by the CHEMP algorithm, i.e., $p^{(0)}(x_j = s_k) = 1/\sqrt{M}, 1 \leq k \leq \sqrt{M}$, and the expectation $\mathbb{E}^{(0)}(x_j)$ and the variance $\mathrm{Var}^{(0)}(x_j)$ are calculated by $p^{(0)}(x_j = s_k)$.

Given the computed $\mu_i^{(t)}$ and $\sigma_i^{2(t)}$, $p^{(t)}(x_j = s_k)$ is proportional to $\exp\big(\frac{-(z_j - J_{jj}s_k - \mu_j^{(t)})^2}{2\sigma_j^{2(t)}}\big)$, the log-likelihood ratio (LLR) of symbol x_j is calculated by

$$\begin{aligned} L^{(t)}(x_j = s_k) &= \ln\frac{p^{(t)}(x_j = s_k)}{p^{(t)}(x_j = s_1)} \\ &= \frac{(2(z_j - \mu_j^{(t)}) - J_{jj}(s_k + s_1))(J_{jj}(s_k - s_1))}{2\sigma_j^{2(t)}} \end{aligned} \tag{10}$$

for $k = 1, 2, ..., \sqrt{M}$. Then, the probability of the candidate point s_k for x_j can be expressed as

$$p^{(t)}(x_j = s_k) = \frac{\exp\big(L^{(t)}(x_j = s_k)\big)}{\sum_{i=1}^{\sqrt{M}} \exp\big(L^{(t)}(x_j = s_k)\big)}, \tag{11}$$

which completes a single iteration about updating $p^{(t)}(x_j = s_k)$. To summarize, given $p^{(t-1)}(x_j = s_k), 1 \leq j \leq 2K, 1 \leq k \leq \sqrt{M}$, the CHEMP algorithm works at the t-th iteration in the following steps:

1) Calculate the expectation $\mathbb{E}^{(t)}(x_j)$ and the variance $\mathrm{Var}^{(t)}(x_j)$ by $p^{(t-1)}(x_j = s_k), 1 \leq k \leq \sqrt{M}$.
2) Update the mean $\mu_i^{(t)}$ and variance $\sigma_i^{2(t)}$ of g_i.
3) Calculate the LLR of symbol x_j through the mean $\mu_i^{(t)}$ and variance $\sigma_i^{2(t)}$.
4) Obtain the probability $p^{(t)}(x_j = s_k)$ of candidate points from LLR $L^{(t)}(x_j = s_k)$.

Finally, after T iterations, the decoding solution $\widehat{x}_j$ can be obtained by choosing the candidate point with the largest probability.

III. The Proposed CHEMP Receiver

In this section, the two stages of the proposed ECHEMP algorithm are presented, namely, the optimization of the initial probability distribution and the approximated probability updating mechanism for detection symbols, which lead to performance improvement and complexity reduction respectively.

A. The Optimization of the Initial Probability Distribution

Theoretically, the selection of the initial probability setup of x_j plays an important role in decoding performance. Specifically, if all the initial probabilities of these real constellation points are evenly distributed, it corresponds to setting the detection symbols $\mathbf{x}^{(0)}$ as $\mathbf{0}$ at the beginning of the algorithm, which may be far away from the final solution. For this reason, it is encouraged to perform estimations about x_j with a well chosen initial probability distribution so that more information can be introduced to serve for the symbol detection. Here, we propose to initialize the probability of candidate points by using discrete Gaussian distribution, where the candidate point closer to the estimated mean η_j of x_j, is assigned with a larger probability.

Specifically, the discrete Gaussian distribution over $\mathcal{X}$ is defined as

$$p^{(0)}(x_j = s_k) = \frac{e^{-\frac{1}{2\rho^2}||s_k - \eta_j||^2}}{\sum_{k\in[1,\sqrt{M}]} e^{-\frac{1}{2\rho^2}||s_k - \eta_j||^2}}. \tag{12}$$

Here, $p^{(0)}(x_j = s_k)$ is the probability of candidate point s_k for x_j. η_j and ρ^2 are the mean and variance of the discrete Gaussian distribution. The initial probability distribution can be adjusted by variance ρ^2. In this paper, the variance $\rho^2 = 4$ is used for calculation. η_j in (12) is determined by the initial vector $x_j^{(0)}$ which is closer to the final solution, i.e., $\eta_j = x_j^{(0)}$. Then, we estimate the initial detection symbols $\mathbf{x}^{(0)}$ under channel hardening phenomenon.

In theory, with the increment of antennas, the diagonal elements of $\mathbf{H}^T\mathbf{H}$ becomes more and more dominated. As can be seen clearly, Fig.1 shows the amplitudes of the Gram matrix $\mathbf{H}^T\mathbf{H}$ with different antenna numbers. This indicates that the Gram matrix $\mathbf{H}^T\mathbf{H}$ is diagonally dominant in the case of large scale MIMO systems, where the difference between

the diagonal matrix $\mathbf{D} = \mathrm{diag}(\mathbf{H}^T\mathbf{H})$ and the Gram matrix $\mathbf{H}^T\mathbf{H}$ is getting smaller, i.e.

$$\mathbf{D} = \lim_{K\to\infty} \mathbf{H}^T\mathbf{H} \approx \mathrm{diag}(\mathbf{H}^T\mathbf{H}). \tag{13}$$

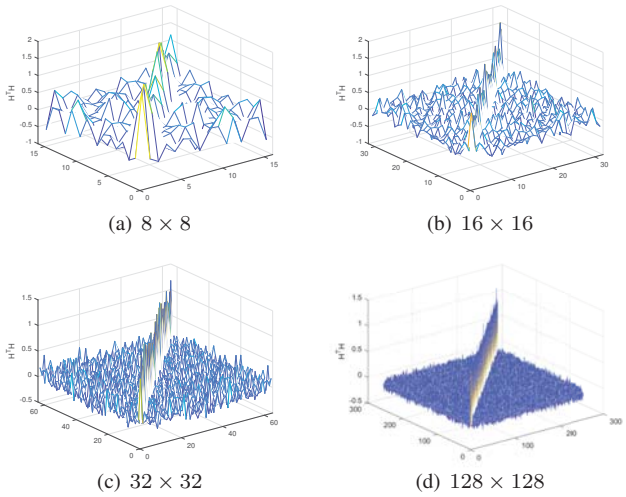

(a) 8×8 (b) 16×16

(c) 32×32 (d) 128×128

Fig. 1: Magnitude plots of $\mathbf{H}^T\mathbf{H}$ for MIMO systems with different number of antennas

According to this approximation, the optimized initial detection symbols $\mathbf{x}^{(0)}$ can be estimated by

$$\mathbf{x}^{(0)} = N\mathbf{D}^{-1}\mathbf{z}. \tag{14}$$

Then, $\mathbf{x}^{(0)}$ obtained by (14) is used to update the initial probability $p^{(0)}(x_j = s_k)$. Note that since $\mathbf{D}$ is a diagonal matrix, the computational complexity of $\mathbf{x}^{(0)}$ is only increased by $2K$ multiplications.

The estimation of the initial probability $p^{(0)}(x_j = s_k)$ is summarized as follows.

1) Use diagonal matrix $\mathbf{D} = \mathrm{diag}(\mathbf{H}^T\mathbf{H})$ to approximate gram matrix $\mathbf{H}^T\mathbf{H}$ under channel hardening.
2) Estimate the initial detection symbols $\mathbf{x}^{(0)}$ using $\mathbf{D} = \mathrm{diag}(\mathbf{H}^T\mathbf{H})$.
3) Compute the initial probability $p^{(0)}(x_j = s_k)$ by the discrete Gaussian distribution in (12).

Finally, under the channel hardening phenomenon, the estimated initial detection symbols $\mathbf{x}^{(0)}$ is taken as the mean of the discrete Gaussian distribution. Therefore, at the same number of iterations, the initial probability $p^{(0)}(x_j = s_k)$ is improved, so as to a better decoding performance.

B. The Probability Updating Mechanism

Firstly, for a system with M-QAM, $\mathbb{E}(x_j)$ and $\mathrm{Var}(x_j)$ in (8) and (9) can be written as

$$\mathbb{E}(x_j) = s_1 p(x_j = s_1) + ... + s_{\sqrt{M}} p(x_j = s_{\sqrt{M}}), \tag{15}$$

$$\mathrm{Var}(x_j) = s_1^2 p(x_j = s_1) + ... + s_{\sqrt{M}}^2 p(x_j = s_{\sqrt{M}}) - \mathbb{E}^2(x_j). \tag{16}$$

In the original CHEMP algorithm, all $\sqrt{M}$ constellation points of x_j are used to update $\mathbb{E}(x_j)$ and $\mathrm{Var}(x_j)$ as shown in (15) and (16), respectively. As for the update of the probability of one symbol, there are $(2K-1)$ computations for $\mathbb{E}(x_j)$ and $\mathrm{Var}(x_j)$, respectively.

It is not difficult to find that when the probability of a candidate point s_k of x_j is much larger than the probability of other candidate points s_k,

$$p(x_j = s_k) > \sum_{l\neq k} p(x_j = s_l), 1 \le k, l \le \sqrt{M}, \tag{17}$$

the decoding result is most likely unchanged with the increase of the number of iterations. Actually, the probabilities of candidate points for some symbol x_j quickly meets the condition in (17) after a few iterations.

As a result, the approximated probability updating mechanism sets a probability threshold p_{th}. When the probabilities of candidate points

$$\max_{s\in\mathcal{X}} p^{(t)}(x_j = s_k) > p_{th}, 1 \le k \le \sqrt{M}, \tag{18}$$

the same x_j is obtained for both the original CHEMP algorithm and the proposed mechanism. The set $\mathcal{S}$ is used to store the subscript of the detection symbol x_j that meets the condition (18).

Therefore, the proposed mechanism reduces the computations of $\mathbb{E}(x_j)$ and $\mathrm{Var}(x_j)$. At the t-th iteration, we can rewrite (8) as

$$\mu_i^{(t)} = \mathbb{E}^{(t)}(g_i) = \sum_{j=1, j\neq i}^{2K} J_{ij}\hat{\mathbb{E}}(x_j). \tag{19}$$

$\hat{\mathbb{E}}(x_j)$ in (19) represents $\mathbb{E}^{(t-1)}(x_j)$ when j belongs to the set $\mathcal{S}$. Otherwise, $\hat{\mathbb{E}}(x_j)$ represents $\mathbb{E}^{(t)}(x_j)$, which is calculated from (15). Similarly, $\sigma_i^{2(t)}$ in (9) can also be obtained. For example, there are m elements in the set $\mathcal{S}$ at the t-th iteration. Then only $(2K-m-1)$ calculations of $\mathbb{E}(x_j)$ and $\mathrm{Var}(x_j)$ need to be computed in the next iteration. It is worth noting that the calculations of $\mathbb{E}(x_j)$ and $\mathrm{Var}(x_j)$ exclude the elements of set $\mathcal{S}$ in each iteration. Furthermore, the elements in set $\mathcal{S}$ also reduce other calculations during iteration.

It is concluded that the selection of appropriate probability threshold p_{th} has significant influence on the decoding performance. The optimization of the probability threshold will be further investigated in our future work.

Damping is an efficient way to improve algorithm performance. The damping factor is obtained by simulation. Specifically, the probability at the t-th iteration is represented by $\tilde{p}^t(x_j = s_k), 1 \le k \le \sqrt{M}$. Then, the probability at the end of t-th iteration is

$$p^{(t)}(x_j = s_k) = (1-\Delta)\tilde{p}^{(t)}(x_j = s_k) + \Delta p^{(t-1)}(x_j = s_k) \tag{20}$$

with $\Delta \in [0, 1)$.

Overall, based on the optimization of the initial probability distribution and the approximated probability updating mechanism, the proposed ECHEMP algorithm for M-QAM is described in *Algorithm* 1. The initial probability $p^{(0)}(x_j = s_k)$ of detection symbol x_j is described in lines 1 to 5 of the algorithm. The ECHEMP algorithm increases the

probability threshold judgment in lines 14 to 16 compared to the original CHEMP algorithm. At the end of the t-th iteration of the detection algorithm described above, we obtain the probabilities of the j-th user's symbol information, $p^{(t)}(x_j = s_k), 1 \le k \le \sqrt{M}$. Finally, the candidate point with the largest probability $p^{(t)}(x_j = s_k)$ is the final solution of x_j.

Algorithm 1 The Proposed ECHEMP Algorithm

Input: $\mathbf{z}, \mathbf{J}, \sigma_v^2, \rho, \Delta, p_{th}, \mathcal{S} = \varnothing, T$

1: $\mathbf{D} = \mathrm{diag}(\mathbf{H}^T\mathbf{H})$
2: $\mathbf{x}^{(0)} = \mathbf{D}^{-1}\mathbf{z}$
3: **for** $j = 1$ to $2K$ **do**
4: $\quad p^{(0)}(x_j = s_k) = \dfrac{e^{-\frac{1}{2\rho^2}||s_k - \eta_j||^2}}{\sum_{k\in[1,\sqrt{M}]} e^{-\frac{1}{2\rho^2}||s_k - \eta_j||^2}}.$
5: **end for**
6: **for** $t = 1$ to T **do**
7: $\quad$ **for** $j = 1$ to $2K$ **do**
8: $\quad\quad$ **if** $j \notin \mathcal{S}$ **then**
9: $\quad\quad\quad$ compute $\mu_j^{(t)}$ according to (8)
10: $\quad\quad\quad$ compute $\sigma_j^{2(t)}$ according to (9)
11: $\quad\quad\quad$ compute $L^{(t)}(x_j = s_k)$ according to (10)
12: $\quad\quad\quad$ compute $\tilde{p}^{(t)}(x_j = s_k)$ according to (11)
13: $\quad\quad\quad$ compute $p^{(t)}(x_j = s_k)$ according to (20)
14: $\quad\quad\quad$ **if** $p^{(t)}(x_j = s_k) > p_{th}$ **then**
15: $\quad\quad\quad\quad$ save the symbol subscript of j-th user in set $\mathcal{S}$
16: $\quad\quad\quad$ **end if**
17: $\quad\quad$ **else**
18: $\quad\quad\quad \mu_j^{(t)} = \mu_j^{(t-1)}$
19: $\quad\quad\quad \sigma_j^{2(t)} = \sigma_j^{2(t-1)}$
20: $\quad\quad\quad L^{(t)}(x_j = s_k) = L^{(t-1)}(x_j = s_k)$
21: $\quad\quad\quad p^{(t)}(x_j = s_k) = p^{(t-1)}(x_j = s_k)$
22: $\quad\quad$ **end if**
23: $\quad$ **end for**
24: **end for**
25: **for** $j = 1$ to $2K$ **do**
26: $\quad$ compute $\widehat{x}_j$ according to (7)
27: **end for**

Output: $\widehat{\mathbf{x}} = [\widehat{x}_1, ..., \widehat{x}_{2K}]$

IV. SIMULATION RESULTS

To demonstrate the superiority of the proposed ECHEMP algorithm in decoding trade-off, its bit error rate (BER) performance in large-scale MIMO detection is presented. Fig. 2 shows the BER performance of ECHEMP algorithm with $N = 128, K = 128, \Delta = 0.3, p_{th} = 0.98$, compared to the Gaussian tree approximation algorithm (GTA) in [11] and the original CHEMP algorithm under 4-QAM. For a better comparison, the two stages contained in the ECHEMP algorithm, the optimization of the initial probability distribution and the approximated probability updating mechanism, are also given respectively. The approximated probability updating mechanism reduces the complexity by the probability threshold, leading to a better decoding trade-off.

Fig. 3 shows the BER performance of the proposed ECHEMP algorithm, the original CHEMP algorithm and the PA-MPD algorithm in [8]. As can be seen clearly, the ECHEMP algorithm has better decoding performance than the original CHEMP algorithm and the PA-MPD algorithm. Fig. 4 shows the BER performance of the proposed ECHEMP algorithm and the original CHEMP algorithm with different K for a fixed $N = 128$ under 16-QAM.

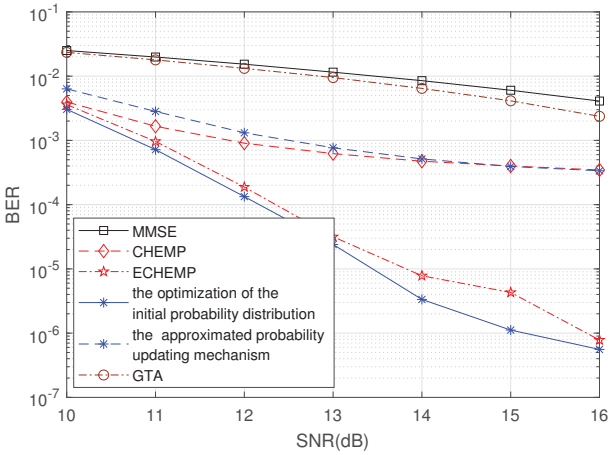

Fig. 2: BER performance of MMSE detector, the original CHEMP, GTA [11] and ECHEMP algorithm(9 iterations)

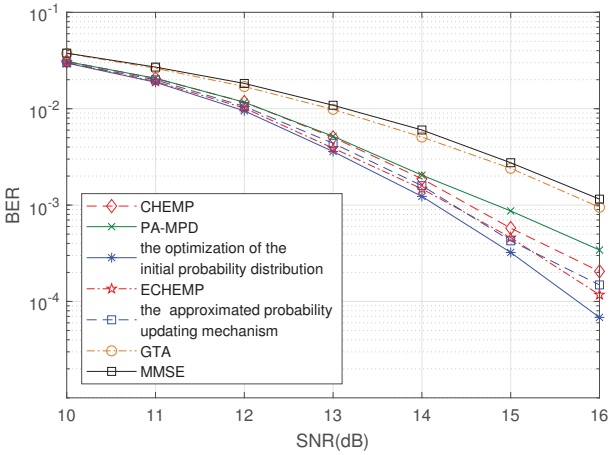

Fig. 3: BER performance of MMSE detector, the original CHEMP, PA-MPD [8], GTA [11] and ECHEMP algorithm with $N = 128$, $K = 64$, $\Delta = 0.26$, $p_{th} = 0.98$, 16-QAM

Here, the complexities of the ECHEMP algorithm and the CHEMP algorithm are also analyzed. Specifically, The computational complexity is analyzed in terms of the numbers of real-valued multiplications and additions. In Table I, we present the complexity comparison between the original CHEMP algorithm and the ECHEMP algorithm under M-QAM. The number of multiplications and additions in the

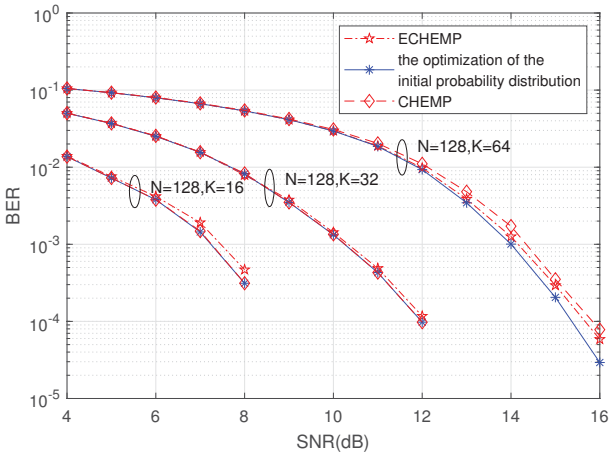

Fig. 4: BER performance of CHEMP algorithm, the ECHEMP algorithm for different values of K for a fixed N = 128 under 16-QAM

ECHEMP algorithm consists of two parts. The number of the first part of multiplications is $(2\sqrt{M}+1)(2K-1)2K$, which is the calculations of the mean and variance of g_i. The number of the second part is $5\sqrt{M}\times 2K$, which is the calculations of the LLR and $p^{(t)}(x_j = s_k)$. Similarly, the number of additions is $((2\sqrt{M}-1)(2K-1)+5\sqrt{M})2K$.

After t iterations, in the original CHEMP algorithm, the number of multiplications and additions are $((2\sqrt{M}+1)(2K-1)+5\sqrt{M})2Kt$ and $((2\sqrt{M}-1)(2K-1)+5\sqrt{M})2Kt$, respectively. Because the calculations of μ_i and σ_i^2 exclude the elements of set $\mathcal{S}$, the proposed ECHEMP algorithm can reduce the complexity to $((2\sqrt{M}+1)(2K-1)+5\sqrt{M})\sum(2K-m)$ and $((2\sqrt{M}-1)(2K-1)+5\sqrt{M})\sum(2K-m)$. Note that m refers to the number of symbols x_j that meet the probability threshold condition (18). The detailed numerical comparisons between the ECHEMP algorithm and the CHEMP algorithm under 16-QAM are shown in Table II.

TABLE I: The complexity comparison between ECHEMP algorithm and CHEMP algorithm

	original CHEMP	proposed ECHEMP
multiplications	$((2\sqrt{M}+1)(2K-1)$ $+5\sqrt{M})2Kt$	$((2\sqrt{M}+1)(2K-1)$ $+5\sqrt{M})\sum(2K-m)$
additions	$((2\sqrt{M}-1)(2K-1)$ $+5\sqrt{M})2Kt$	$((2\sqrt{M}-1)(2K-1)$ $+5\sqrt{M})\sum(2K-m)$

TABLE II: Numerical comparison

	original CHEMP	proposed ECHEMP
multiplications	1339776	897836
additions	1047168	701748

For antenna configuration of $K = 16$ and $N = 128$ with 16-QAM, the selection of the probability threshold here is 0.98, $p_{th} = 0.98$. Although the chosen probability threshold is extremely high, the comparison of the number of multiplications and additions can show that the proposed ECHEMP algorithm has achieved a large amount of calculation reduction. The ECHEMP algorithm can achieve about 33% complexity reduction compared to the CHEMP algorithm.

V. CONCLUSION

In this paper, the enhanced CHEMP (ECHEMP) algorithm is proposed, which not only reduces the computational load but also improves the decoding performance. We obtain better convergence performance by using the discrete Gaussian distribution to optimize the initial probability distribution. Then, the complexity of the original CHEMP algorithm is effectively reduced through the probability threshold. Consequently, the proposed ECHEMP algorithm is able to achieve a better decoding trade-off.

ACKNOWLEDGMENT

This work was supported in part by the National Natural Science Foundation of China (Grants No. 61801216), the Natural Science Foundation of Jiangsu Province under Grant BK20180420.

REFERENCES

[1] L. Liu, C. Yuen, Y. L. Guan, Y. Li, and C. Huang, "Gaussian Message Passing for Overloaded Massive MIMO-NOMA," *IEEE Transactions on Wireless Communications*, vol. 18, no. 1, pp. 210–226, 2019.

[2] C. Ling, "On the Proximity Factors of Lattice Reduction-Aided Decoding," *IEEE Transactions on Signal Processing*, vol. 59, no. 6, pp. 2795–2808, 2011.

[3] L. Dai, X. Gao, X. Su, S. Han, C. I, and Z. Wang, "Low-Complexity Soft-Output Signal Detection Based on Gauss–Seidel Method for Uplink Multiuser Large-Scale MIMO Systems," *IEEE Transactions on Vehicular Technology*, vol. 64, no. 10, pp. 4839–4845, 2015.

[4] G. Peng, L. Liu, P. Zhang, S. Yin, and S. Wei, "Low-Computing-Load, High-Parallelism Detection Method Based on Chebyshev Iteration for Massive MIMO Systems With VLSI Architecture," *IEEE Transactions on Signal Processing*, vol. 65, no. 14, pp. 3775–3788, 2017.

[5] M. Wu, B. Yin, G. Wang, C. Dick, J. R. Cavallaro, and C. Studer, "Large-Scale MIMO Detection for 3GPP LTE: Algorithms and FPGA Implementations," *IEEE Journal of Selected Topics in Signal Processing*, vol. 8, no. 5, pp. 916–929, 2014.

[6] W. Fukuda, T. Abiko, T. Nishimura, T. Ohgane, Y. Ogawa, Y. Ohwatari, and Y. Kishiyama, "Low-Complexity Detection Based on Belief Propagation in a Massive MIMO System," in *2013 IEEE 77th Vehicular Technology Conference (VTC Spring)*, 2013, pp. 1–5.

[7] T. L. Narasimhan and A. Chockalingam, "Channel Hardening-Exploiting Message Passing (CHEMP) Receiver in Large-Scale MIMO Systems," *IEEE Journal of Selected Topics in Signal Processing*, vol. 8, no. 5, pp. 847–860, 2014.

[8] H. Zhu, J. Lin, and Z. Wang, "Reduced complexity message passing detection algorithm in large-scale MIMO systems," in *2017 9th International Conference on Wireless Communications and Signal Processing (WCSP)*, 2017, pp. 1–5.

[9] X. Tan, W. Xu, K. Sun, Y. Xu, Y. Be'ery, X. You, and C. Zhang, "Improving Massive MIMO Message Passing Detectors With Deep Neural Network," *IEEE Transactions on Vehicular Technology*, vol. 69, no. 2, pp. 1267–1280, 2020.

[10] J. Zeng, J. Lin, and Z. Wang, "Low Complexity Message Passing Detection Algorithm for Large-Scale MIMO Systems," *IEEE Wireless Communications Letters*, vol. 7, no. 5, pp. 708–711, 2018.

[11] J. Goldberger and A. Leshem, "MIMO Detection for High-Order QAM Based on a Gaussian Tree Approximation," *IEEE Transactions on Information Theory*, vol. 57, no. 8, pp. 4973–4982, 2011.